frontiers | Frontiers in Neural Circuits

TYPE Original Research
PUBLISHED 25 April 2025
DOI 10.3389/fncir.2025.1563401

OPEN ACCESS

EDITED BY
Xiangmin Xu,
University of California, Irvine, United States

REVIEWED BY
Juan Saez,
Universidad de Valparaiso, Chile
Yael Grosjean,
Centre National de la Recherche Scientifique (CNRS), France

*CORRESPONDENCE
Dafni Hadjieconomou
✉ dafni.hadjieconomou@icm-institute.org
Diane K. O'Dowd
✉ dkodowd@uci.edu
Jorge M. Campusano
✉ jmcampus@uc.cl

†These authors have contributed equally to this work

RECEIVED 19 January 2025
ACCEPTED 31 March 2025
PUBLISHED 25 April 2025

CITATION
Fuenzalida-Uribe N, Hidalgo S, Silva B, Gandhi S, Vo D, Zamani P, Holmes TC, Sayin S, Grunwald Kadow IC, Hadjieconomou D, O'Dowd DK and Campusano JM (2025) The innexin 7 gap junction protein contributes to synchronized activity in the *Drosophila* antennal lobe and regulates olfactory function.
Front. Neural Circuits 19:1563401.
doi: 10.3389/fncir.2025.1563401

The innexin 7 gap junction protein contributes to synchronized activity in the *Drosophila* antennal lobe and regulates olfactory function

Nicolás Fuenzalida-Uribe[1,2†], Sergio Hidalgo[1,3†], Bryon Silva[1,4†], Saurin Gandhi[5], David Vo[5], Parham Zamani[5], Todd C. Holmes[6], Sercan Sayin[7], Ilona C. Grunwald Kadow[8], Dafni Hadjieconomou[4]*, Diane K. O'Dowd[5]* and Jorge M. Campusano[1]*

[1]Laboratorio Neurogenética de la Conducta, Facultad de Ciencias Biológicas, Pontificia Universidad Católica de Chile, Santiago, Chile, [2]Institute of Neurobiology, University of Puerto Rico- Medical Sciences Campus, San Juan, Puerto Rico, [3]Department of Integrative Physiology and Neuroscience, Washington State University, Pullman, Washington, DC, United States, [4]Sorbonne Université, Inserm, CNRS, Hôpital Pitié-Salpêtrière, Institut du Cerveau-Paris Brain Institute (ICM), Paris, France, [5]Department of Developmental and Cell Biology, University of California Irvine, Irvine, CA, United States, [6]Department of Physiology and Biophysics, and Center for Neural Circuit Mapping, University of California Irvine, Irvine, CA, United States, [7]Department of Biology, University of Konstanz, Konstanz, Germany, [8]Faculty of Medicine, University of BonnInstitute of Physiology, Bonn, Germany

In the mammalian olfactory bulb (OB), gap junctions coordinate synchronous activity among mitral and tufted cells to process olfactory information. In insects, gap junctions are also present in the antennal lobe (AL), a structure homologous to the mammalian OB. The invertebrate gap junction protein ShakB contributes to electrical synapses between AL projection neurons (PNs) in *Drosophila*. Other gap junction proteins, including innexin 7 (Inx7), are also expressed in the *Drosophila* AL, but little is known about their contribution to intercellular communication during olfactory information processing. In this study, we report spontaneous calcium transients in PNs grown in cell culture that are highly synchronous when these neurons are physically connected. RNAi-mediated knockdown of Inx7 in cultured PNs blocks calcium transient neuronal synchronization. *In vivo*, downregulation of Inx7 in the AL impairs both vinegar-induced electrophysiological calcium responses and behavioral responses to this appetitive stimulus. These results demonstrate that Inx7-encoded gap junctions functionally coordinate PN activity and modulate olfactory information processing in the adult *Drosophila* AL.

KEYWORDS

***Drosophila*, olfactory information, gap junction, innexin, calcium dynamics**

Introduction

The organization and operation of olfactory circuits are highly conserved between vertebrates and invertebrates. Olfactory information is first received by the olfactory receptor neurons (ORNs) that project to discrete glomerular structures in the olfactory bulb (OB) in mammals and the antennal lobe (AL) in insects. Within glomeruli, olfactory information is integrated and then transmitted to higher processing centers, including cortical areas in mammals and the mushroom

bodies (MBs) in insects, where olfactory memories can be formed and stored (Ache and Young, 2005; Vosshall and Stocker, 2007; Grabe and Sachse, 2018; Fabian and Sachse, 2023). In addition to the anatomical organization, the similarities between vertebrate and invertebrate olfactory systems extend to the cellular and molecular mechanisms responsible for processing odorant information. These cellular and molecular olfactory mechanisms, including those used in invertebrate models, are not completely understood.

Electrical synapses, formed by gap junctions, are important players in neuronal communication, information processing, and ultimately brain function (Connors and Long, 2004; Nagy et al., 2018). This type of cell communication underlies most of the coupled activity observed within neural circuits, including the mammalian olfactory system. For instance, the synchronized activity recorded between the mitral and the tufted cells of the OB glomeruli, which is involved in the processing of olfactory information and stimuli gain, is mediated by electrical synapses (Chen et al., 2009; Christie et al., 2005; Ma and Lowe, 2010; Schoppa and Westbrook, 2001). Similarly, electrical synchronization within the AL is also thought to be important in pheromone and food-related odor processing in insects (Das et al., 2017; Martin et al., 2013; Kay, 2015; Stopfer and Laurent, 1999).

Gap junctions are formed by specific proteins: in vertebrates, they are encoded by two gene families, connexins and pannexins, while in invertebrates, gap junctions are formed by just one family of proteins, the innexins (Bauer et al., 2005; Beyer and Berthoud, 2018). Out of the eight innexins identified in the *Drosophila melanogaster* genome (*inx 1–8*), four of them (*inx5*, *inx6*, *inx7*, and *shakB*, also known as *inx8*) show detectable mRNA levels in neurons in the pupal and adult fly brain. Notably, *lnx7* and *shakB* innexins exhibit the highest transcript levels (Stebbings et al., 2002). Consistent with these expression studies, it has been shown that *shakB* plays a role in developing *Drosophila* optic lobe lamina (Curtin et al., 2002). Importantly, ShakB shows the highest expression in mature fly AL (Stebbings et al., 2002; Ammer et al., 2022), which is consistent with the finding that this innexin mediates electrical synapses between sister PNs and also between pairs of AL lateral neurons (LNs) (Kazama and Wilson, 2009; Yaksi and Wilson, 2010; Huang et al., 2010). Less is known regarding the contribution of other innexins to brain development or function. In this regard, it was demonstrated that Inx7 plays a role in axon guidance and nervous system development (Ostrowski et al., 2008). In addition to this, it was reported that Inx7 forms heterotypic gap junctions between two modulatory neurons in MB that contribute to olfactory memory (Wu et al., 2011).

Here we focus on the functional role that Inx7 plays in *Drosophila's* olfactory function. Our data demonstrate that the knockdown of Inx7 in AL PNs decouples correlated calcium activity between physically connected PNs grown in cell culture. *In vivo*, evoked calcium signals in *Drosophila* AL by vinegar exposure are impaired by the knockdown of Inx7 in this fly brain region. Furthermore, we show that Inx7 expression in AL PNs is required for olfactory behavioral responses to vinegar exposure. These results reveal a previously unrecognized role for Inx7 gap junctions in the integration of olfactory sensory information in flies.

Materials and methods

Flies

To identify antennal lobe PNs, we used the GH146-gal4 driver [w^{1118}; *GH146-Gal4* (Stocker et al., 1997)]. This gal4 line drives the expression of genes in most but not all AL PNs (~2/3 of the entire adult AL PN population) (Stocker et al., 1997; Jefferis et al., 2001). It has been shown that in very early pupae, this gal4 line drives the expression of genes in other brain regions such as the optic lobe, although as animals develop, the expression in regions other than the AL decreases (Xie et al., 2021). Flies bearing the GH146-gal4 transgene were crossed with flies containing a UAS-GFP transgene. In F1 of this cross, it is possible to detect GFP expression in the AL (see Figure 1A). Strains were obtained from the Bloomington *Drosophila* Stock Center (BDSC, Indiana University, IN) (strains # 30026 and 1,521, respectively). Recombinant animals homozygous for these two transgenes were obtained (from here on GH146, GFP) and were crossed to a strain that allows the expression of an RNAi targeting Inx7 (RNAi^{inx7}) under the control of UAS (w^{1118}; *UAS-RNAI*^{inx7}), which was obtained from the (Vienna *Drosophila* Resource Center, VDRC, Vienna, Austria) (strain ID#22949, which we called Inx7-KD-a-PN).

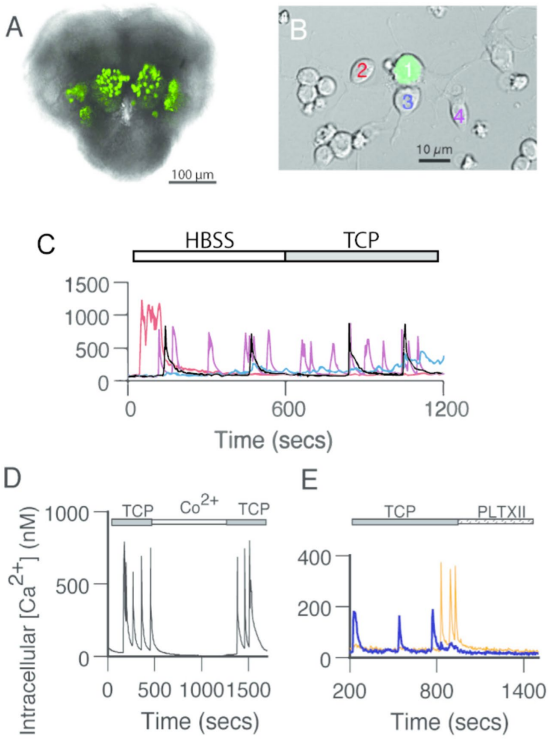

FIGURE 1
GFP-positive PNs generate spontaneous calcium transients independent of fast chemical synaptic transmission. **(A)** GFP-positive antennal lobe PNs in the brain of a late-stage pupa. Bright-field image with a fluorescent overlay of the anterior face in the brain of a GH146 > GFP pupa at ~72 h after pupation. **(B)** GFP-positive PNs surrounded by GFP-negative neurons in dissociated cell culture at 3 DIV. Fluorescent mask projected on a Nomarski image. **(C)** Spontaneous calcium transients in GFP-positive PNs recorded in standard saline (HBSS) are not affected by the addition of TCP, a cocktail of drugs that block synaptic transmission (1 µM TTX, 20 µM curare, 10 µM picrotoxin). Traces correspond to the calcium levels in the neurons presented with different colors in **(B)**. **(D)** Addition of cobalt (Co^{2+}, 2 mM) reversibly blocks spontaneous calcium transients. Representative experiment. **(E)** Exposure to an irreversible voltage-gated calcium channel blocker, Plectreurys toxin (PLTXII, 50 nM), inhibits spontaneous calcium transients. In this and all other subsequent figures, intracellular calcium levels were monitored using the ratiometric imaging dye Fura-2 AM. The 340/380 ratios were sampled at 4-s intervals and converted to estimates of intracellular calcium based on a standard calcium curve.

A second RNAi^{inx7} strain was also used for some preliminary experiments (VDRC #22948). In some experiments (see below), *elav-gal4*,w^{1118} animals were used to drive the RNAi^{inx7}. Flies were kept at 18°C throughout their development to diminish the expression of gal4-driven genes. Only 3 days before they were used for experiments, they were brought to room temperature (22°C). For additional experiments, we used the strain ID#50856, obtained from BDSC.

Quantitative PCR experiments

The efficacy of the RNAi^{inx7} line was assessed by qPCR. For these experiments, RNA was prepared from adult fly heads obtained after elav-Gal4,w^{1118} flies were mated with w^{1118};UAS-RNAi^{inx7} animals. RNA obtained from the heads of parental strains was used as a control.

The procedure to carry out PCR was as described (Rojo-Cortes et al., 2022). Briefly, cDNA was prepared from each RNA sample with 2 μg of RNA as the starting material. RT-qPCR was carried out using the 5 × HOTFIREPol® EvaGreen® qPCR Mix Plus Kit (Solis BioDyne) and LightCycler® (Roche) apparatus. PCR parameters were: 94°C for 6 min, followed by 40 cycles of 94°C for 10 s, 56°C for 15 s, and 72°C for 20 s. Primer efficiency was evaluated after a serial dilution of the reaction mix and was calculated as $10^{-1/slope}$. The *ribosomal protein 49* gene was used for RNA quantitation. Primer pairs were designed with MacVector software: RP49F1, 5′-caagggtatcgacaacagagtcg-3′; RP49B1, 5′-tgcaccaggaacttcttgaatcc-3′ (amplicon of 126 bp); and *inx7*F9, 5′-tttggtgactctggctccattc-3′,5′-cgcaggaagaaaaggaacatcc-3′ (amplicon of 287 bp). Analysis of relative gene expression (*inx7* target gene vs. *RP49* reference gene) in knockdowns vs. control lines was calculated according to the $2^{-\Delta\Delta CT}$ method.

Our results show that the two RNAi strains showed differential efficiency at decreasing *inx7* transcript expression: the ID#22949 resulted in a decrease of 85 ± 7% of *inx7* mRNA expression, while the ID#22948 s RNAi strain reduced *inx7* transcript expression to only 50 ± 7% (n = 3 independent experiments per strain). Thus, we decided to work only with the RNAi^{inx7} ID#22949.

Primary neuronal cultures

Primary neuronal cultures were prepared as previously described (Rojo-Cortes et al., 2022; Leyton et al., 2014; Campusano et al., 2007; Jiang et al., 2005), with some modifications as indicated here below. In initial studies, dissociated neuronal cultures were prepared with one pupal brain per culture. Given the small number of PNs found in one brain, cultures contained only a small number of GFP-positive PNs and a much larger population of GFP-negative neurons. The number of GFP-positive PNs counted in 3–4 days *in vitro* (DIV) cultures was 11.9 ± 1.6 per brain (mean ± SEM, n = 39 cultures). This represents a mean recovery rate (assuming ~100 GFP-labeled PNs/brain) of approximately 10–15%. To increase the number of GFP-expressing neurons in our preparation, each culture was prepared from the ALs dissected from two brains (four ALs per culture). Cultures were maintained in a humidified 5% CO2 incubator at 22–24°C, and imaging experiments were performed on cultures from 4 to 8 DIV.

In vitro calcium imaging

Calcium imaging studies were performed as previously reported (Leyton et al., 2014; Campusano et al., 2007). Briefly, cultures were loaded with the calcium indicator dye Fura2-AM (5 mM, Molecular Probes, Eugene OR), in the presence of pluronic acid (0.1%, Invitrogen) in a HEPES-buffered salt solution (HBSS). Cultures were imaged on an inverted Nikon microscope with a 40x, 1.3 numerical aperture, oil immersion objective. Fluorescent illumination was provided by a 150-W Xenon arc lamp, and filters at 340 and 380 nm were used for excitation. All images were acquired at the emission wavelength of 510 nM and recorded every 4 s via a digital CCD camera (Photometrics, Tucson, AZ). Pseudocolor 340/380 ratio images were generated with MetaFluor software version 5.1 (MDS Analytical Technologies, Sunnyvale, CA). Ratiometric values were converted to estimates of intracellular calcium concentration.

Prior to beginning an experiment, each culture was scanned to determine if it contained at least two GFP-positive PNs in close proximity (pairs). PN pairs, either with adjacent cell bodies or overlapping neuritic processes, were found in ~1 out of 5 cultures, and these were selected for calcium imaging. Intracellular calcium levels were evaluated by determining the average signal across neuronal somata. Neurons were included in the data set if a stable recording was maintained for at least 10 min and an increase in the 340/380 ratio greater than 600 nM was induced by exposure to 5 µM ionomycin at the end of the experiment. A calcium transient was defined as an increase in intracellular calcium concentration greater than 60 nM (>5 times baseline noise level) that reaches its peak within 20 s and declines by at least 50% from the peak within 3 min. The transient frequency in each cell was calculated as the number of transients divided by the time of recording. The amplitude of each transient was measured from baseline to peak, and an average value for each cell was calculated (Jiang et al., 2005). When mentioned, the TCP solution was used to block fast chemical neurotransmission. TCP consisted of TTX (1 µM, Alomone Labs, Israel, to block voltage-gated sodium channels), Curare (d-tubocurarine, 20 µM, Sigma, to block nAChRs), and Picrotoxin (PTX, 10 µM, Sigma, to block GABAA receptors). The following drugs were bath-applied in specific imaging experiments: Plectreurys toxin (PLTX-II, 50 nM, Alomone Labs, Israel) and cobalt chloride (Co^{2+}, 2 mM, Sigma).

A cross-correlation function (CCF) was used to evaluate the correlation in time of spontaneous calcium transients in PN pairs in which both cells were active (>80% of the pairs examined). The CCF was evaluated for a time window of at least 10 min, using the routine available in Clampfit9 (Molecular Devices, CA): The data set of one cell was shifted along with the second, one sample at a time, in both directions. Thus, the CCF measured the correlation between the data sets at each time point. The correlation coefficients reported here are the values of the CCF at lag time 0.

In vivo calcium imaging

Female flies (4- to 7-day-old) of the genotype GH146-Gal4,UAS-GCaMP3 were used for these experiments. *In vivo* imaging was made as previously (Bracker et al., 2013). All imaging experiments were conducted using a Leica DM6000FS fluorescent microscope, a 40x water immersion objective, and a Leica DFC360 FX fluorescent

camera, and focusing on the AL plane. Images were acquired using the Leica LAS AF E6000 software for a total recording time of 60s at a rate of 30 frames per second with 4 × 4 binning mode. Time series images were acquired at 256 × 256 pixel resolution at 30 frames per second. For odor delivery, we used a Syntech stimulus controller CS-55 (Syntech) and mass flow controllers. Throughout the experiments, a charcoal-filtered continuous humidified airstream (1 L/min) was delivered through an 8-mm Teflon tube positioned ~10 mm away from the fly antenna. For odor stimulation, odors were delivered into the main airstream by redirecting ~30% of the main airflow for 1 s through a headspace glass vial containing an appropriately diluted odorant. Balsamic vinegar (Alnatura) was diluted in distilled water. To measure the fluorescent intensity change, a region of interest (AL glomeruli) was drawn manually, and the resulting time trace value was used for data analysis. The relative change in fluorescence intensity was calculated by using the following formula: $\Delta F/F = 100(F_n - F_0)/F_0$, where F_n is the n^{th} frame after stimulation, and F_0 is the average basal fluorescence of five frames before stimulation. All data were normalized to background air. For data analysis, we used the peak maximum value of the response to stimulation. The pseudocolored images were generated using ImageJ. All data processing and statistical tests were conducted using Excel and GraphPad Prism software, respectively.

Spherical treadmill behavioral assay

The spherical treadmill assay, the online speed data acquisition rate, and offline calculations were performed as reported (Sayin et al., 2019). In brief, a tethered female fly was transferred onto the treadmill and assayed after a 3-min period of acclimatization. The assay consisted of 10 consecutive trials of vinegar odor exposure, which were separated by intervals of 60 s. A custom-made PTFE (Teflon) tube with a 4 mm diameter, fixed at ~3 mm distance from the tethered fly, was used for the delivery of the appetitive olfactory stimulus. The airspeed was set to 100 mL/min via a Natec Sensors mass-flow controller. The balsamic vinegar solution was prepared daily at a 20% v/v dilution in 100 mL Schott bottles. Each trial was recorded for a minimum of 52 s. The recording was divided into pre-stimulation (20 s), stimulation (12 s), and post-stimulation (30 s) periods, and the recorded speed data were downsampled to 10 Hz by summation. The average running activity was measured as the fraction of time where flies showed running speeds higher than 0 mm/s while being stimulated with the odor. A stop was defined as flies not moving (0 mm/s) for at least 100 ms. Data were visualized with matplotlib (1.4.2) and graphed as average run speed (mm/s).

Olfactory preference test

Flies were placed in starvation conditions (vial without food, with a filter paper band moistened with water) at 25°C for 24 h before the beginning of the experiment. Groups of 30–50 flies (4- to 6-day-old) were assessed in the olfactory acuity assay, which was carried out as previously described (Rojo-Cortes et al., 2022). The behavior room was kept at 23–26°C with 60–70% relative humidity under dim red light. We used a response index (RI) to express a choice preference for the vinegar odor, calculated by subtracting the number of flies in the air arm from the number of flies in the vinegar arm, divided by the total number of flies. An RI equal to 1 would indicate a 100% preference for the vinegar odor.

Single-fly locomotion

Single-fly locomotion was studied following a protocol previously described (Fuenzalida-Uribe and Campusano, 2018; Hidalgo et al., 2021). Briefly, single flies were placed on a circular white arena (39 mm diameter, 2 mm high) to be video recorded for 3 min at room temperature. Videos were analyzed offline using a video tracking analysis (Buridan-tracker).

Results

Pairs of PNs show correlated calcium transients, which depend on Inx7 expression

Spontaneous calcium activity has been previously reported in cultured *Drosophila* neurons (Campusano et al., 2007; Jiang et al., 2005). To examine whether cultured AL PNs also show spontaneous activity, we monitored calcium concentration under basal conditions using the ratiometric intracellular calcium indicator, Fura-2. AL PNs, identified by cell-specific GFP expression, show calcium transients (Figures 1A–C) such as those observed in Kenyon cells (KCs) (Campusano et al., 2007; Jiang et al., 2005). Calcium signals vary in frequency and waveforms and are not exclusive to AL PNs, as surrounding (GFP-negative) neurons also display these transients (Figure 1C).

To characterize the nature of the spontaneous calcium transients observed in AL PNs in culture, we performed recordings under different conditions (Figures 1C–E). The calcium transients observed in PNs are still present upon exposure to fast-synaptic blockers (TTX, Curare, and Picrotoxin; TCP), suggesting that they are independent of chemical synapses (Figure 1C). Bath application of either Co^{2+} or PLTXII, an insect-specific calcium channel antagonist (Campusano et al., 2007; Jiang et al., 2005), completely abolishes these spontaneous events. These data indicate that calcium transients depend on the activity of PLTXII-sensitive voltage-gated calcium channels (Figures 1D,E).

Although the AL PNs represent a small subset of the total cell population in culture, from time to time we observed pairs of GFP-positive neurons in direct physical contact (Figures 2A–C). The calcium transients in most of these pairs show a high degree of correlation over time under basal recording conditions (Figures 2A,A'). Furthermore, the correlated activity persists in the presence of TCP (Figure 2A'), suggesting that it is independent of chemical synapses.

While the majority of the PN-PN pairs consisted of cells in contact only through their neurites, others were in contact at the level of their cell bodies (Figures 2B,C). We evaluated whether the site of contact influences the degree of correlated activity between PN-PN pairs in culture using a cross-correlation function (CCF). This approach describes the probability of coincidence detection of a calcium transient in one cell while a transient is observed in the second cell in the pair. CCF values close to one indicate a high coincidence of transients between two cells in the pair. The CCF analysis for PN pairs connected only by neurites (e.g., traces shown in Figure 2B') shows a

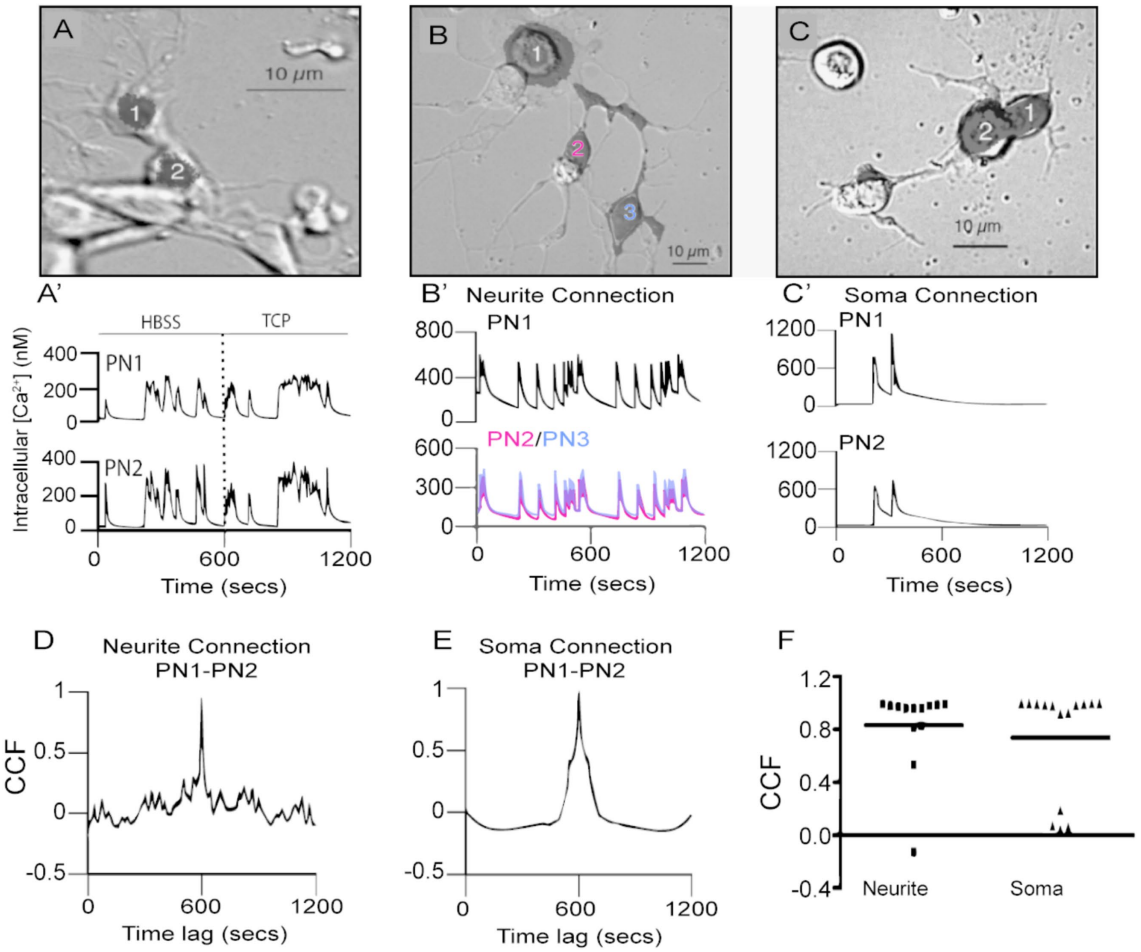

FIGURE 2
Spontaneous calcium transients are highly correlated in time in PN-PN pairs connected by neurites or cell bodies. **(A)** A pair of physically connected GFP-positive PNs in dissociated cell culture at 5 DIV. Fluorescent mask (shaded black) projected on Nomarski image. **(A')** PN1 and 2 generate spontaneous calcium transients that are highly correlated in time in HBSS. Correlated calcium transients in the pair persist following the addition of TCP to block fast chemical synaptic transmission. **(B)** Three PNs in contact through neuritic processes that were regenerated in culture. **(B')** PN1, 2, and 3, connected by newly regenerated neurites PN2 in red and PN3 in blue, **(B)**, have spontaneous calcium transients that are highly correlated in time. **(C)** Two PNs' in contact with their cell bodies. Fluorescent masks (shaded black) projected on Nomarski images. **(C')** Correlated spontaneous calcium transients in PN1 and PN2 **(C)** in contact with their somas. CCF for traces shown in **(B',D)** and in **(C',E)** exhibit a peak value close to 1 at lag time 0. **(F)** Comparison of CCF between pairs of PNs connected through neurites or somas shows no difference between these two situations ($p > 0.33$, Mann–Whitney U-test, two-tailed, $n = 13$ neurite pairs; $n = 14$ soma pairs).

strong correlation as maximal peak values were close to one at lag time 0 (Figure 2D). Similarly, a higher correlation with spontaneous events is found in PNs connected through their soma (Figures 2C,C',E,F). No differences in the correlation coefficients between the two groups are observed (Figures 2F, $p > 0.33$; Mann–Whitney U-test), suggesting that the PN-PN coupled activity is independent of the site of contact between the cells. To determine if the correlated activity was specific to PN-PN pairs, spontaneous calcium transients in PN-GFP-negative pairs that were connected at the somas or through neurons in the same cultures were evaluated. There was little evidence of synchronized activity between PN and non-PN pairs, with correlation coefficients that are significantly lower compared to PN-PN pairs ($p < 0.0001$, Supplementary Figure S1).

Taken together, these results demonstrate correlated spontaneous calcium activity between PN-PN pairs, which is independent of fast chemical neurotransmission and is dependent on PLTXII-sensitive voltage-gated calcium channels.

As the spontaneous coupled activity between PNs is independent of fast chemical synapses, we hypothesized that electrical synapses, mediated by gap junctions, might contribute to the correlated calcium activity. To test this idea, we directed an RNAi against *inx7* to AL PNs to decrease the expression of Inx7 specifically in this cell type. Knockdown of Inx7 expression is effective based on the analysis of transcripts in the knockdown flies (RNAi^{inx7}; 85 ± 7% mRNA decrease as compared to UAS-RNAi^{inx7} parental strain, $n = 3$ independent experiments). Cultures were prepared from the brains of Inx7 knocked-down flies, and these contained PNs in physically connected pairs at a similar frequency as compared to cultures prepared from control flies (Figure 3A). In addition, the PNs found in these cultures generate spontaneous calcium transients such as those detected in control cultures (Figure 3B). Nonetheless, in sharp contrast to control cultures, the calcium transients in PN-PN pairs expressing RNAi^{inx7} show little or no correlated activity in representative calcium transient profiles (Figure 3B). The quantification of all PN-PN pairs expressing

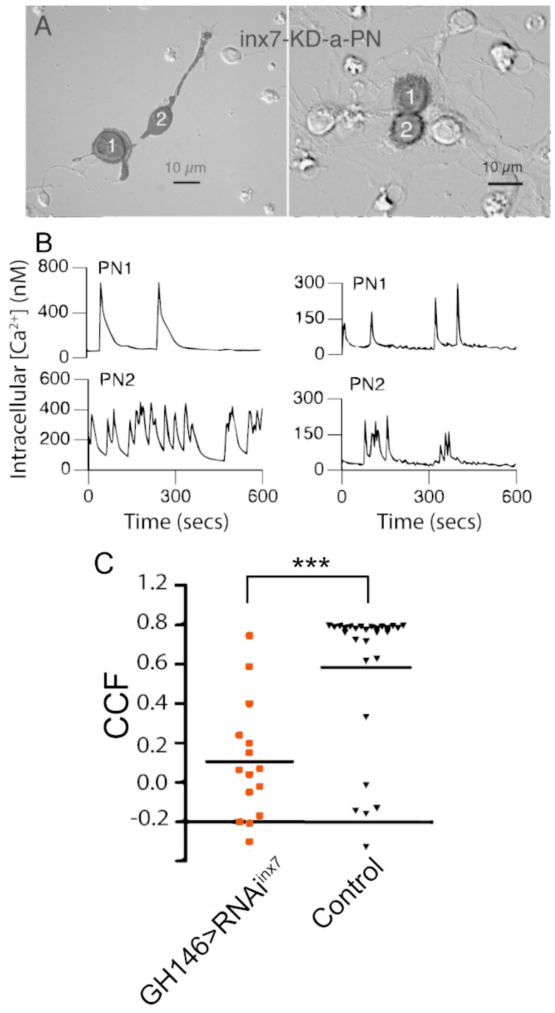

FIGURE 3
Knockdown of Inx7 in PNs reduces the synchronous calcium activity observed in PN-PN pairs. **(A)** Fluorescent mask (shaded in black) projected on Nomarski image is shown for GFP positive PN-PN pairs expressing RNAi^{inx7} in representative experiments. GFP-expressing cells are in contact through neurites (left) or cell bodies (right). **(B)** Calcium transients recorded from PN-PN pairs expressing RNAi^{inx7} in **(A)**. **(C)** Correlation coefficients of all PN-PN pairs in neurons expressing RNAi^{inx7} examined compared to all the PN-PN pairs in cultures made from control flies at the same time (***$p < 0.01$; Kruskal–Wallis ANOVA, GH146 > RNAi^{inx7} $n = 15$ pairs vs. control $n = 28$ pairs).

RNAi^{inx7} evaluated demonstrates that decreasing Inx7 expression decreases correlated calcium activity in physically connected PN-PN pairs (Figure 3C).

Overall, our data show that Inx7 contributes to the correlated calcium activity between cultured *Drosophila* AL PNs.

Evoked calcium activity in AL PNs depends on Inx7

Correlated activity supports odorant processing in both the vertebrate OB and the insect AL (Chen et al., 2009; Kazama and Wilson, 2009). We evaluated whether Inx7 contributes to odor-evoked calcium responses in AL *in vivo*. Flies were exposed to different concentrations of vinegar (an attractive odorant) (Das et al., 2017; Semmelhack and Wang, 2009) while neuronal activity was measured via calcium imaging in AL. Flies that constitutively expressed the genetically encoded calcium sensor GCaMP3 in AL PNs (GH146, GCaMP3, Figure 4) were used as the control strain and were compared to flies recombinant for these transgenes crossed with flies bearing the UAS-RNAi^{inx7} genetic element to knockdown the expression of Inx7.

In response to the odor stimulus (20% vinegar), control flies exhibit a sharp increase in intracellular calcium in AL PNs, as previously described (Figure 4B, black trace) (Semmelhack and Wang, 2009; Strutz et al., 2014). Remarkably, flies expressing the RNAi^{inx7} in AL PNs show an augmented calcium response compared to control animals (Figure 4B, red trace). The vinegar-induced increase in calcium response is consistent across experiments using both 1 and 20% vinegar dilutions (Figure 4C).

These results suggest that Inx7-dependent electrical synapses contribute functionally, not only by synchronizing spontaneous calcium activity between PNs *in vitro,* but also by modulating neuronal activity in AL in response to odorant stimulus *in vivo*.

Decreased Inx7 expression in PNs affects vinegar sensitivity and vinegar-evoked behaviors

The AL is an essential region responsible for organizing and processing odor information before it is sent to higher centers in the *Drosophila* brain (Grabe and Sachse, 2018; Fabian and Sachse, 2023). To study whether the altered calcium activity in the AL, after Inx7 knockdown in PNs, impacts behavioral responses to odorants, we used two behavioral assays.

First, we analyzed the naïve olfactory response to vinegar, an appetitive olfactory stimulus (Semmelhack and Wang, 2009; Strutz et al., 2014). Groups of starved flies were placed in a T-maze apparatus and exposed to 20% vinegar (in one arm) or fresh air (in the other). After a 2-min decision period, the number of flies preferring vinegar or air was quantified, and a response index (RI) was calculated. This assay revealed that downregulation of Inx7 in PNs is sufficient to decrease the RI by 50% compared to control flies (Figure 5A).

We then evaluated the motivation of a fly for an appetitive stimulus (Sayin et al., 2019). To do this, we considered that flies display a preference for an appetitive cue, according to the integration of its internal state and the information provided by the cue. The integration between these two factors has been demonstrated in studies of appetitive memories, where it is reported that flies generate memories only after a starvation period (Krashes et al., 2009). It has also been shown that starved flies persevere in seeking a food source when vinegar scent is repeatedly presented (Sayin et al., 2019). Thus, we hypothesized that alterations in calcium activity in RNAi^{inx7} flies could result in impaired perseverance in seeking a food source. To assess this, we evaluated the locomotor behavior driven by appetitive food and behavior persistence on a spherical treadmill. Single starved flies were placed on top of a spherical treadmill, and the average running speed toward the vinegar cue was quantified after 10 consecutive trials (Figure 5B). Under these conditions, both control and RNAi^{inx7}-expressing flies showed strong attraction toward the first vinegar exposure, evidenced by an increase in speed of movement as compared to the situation when no stimulus was

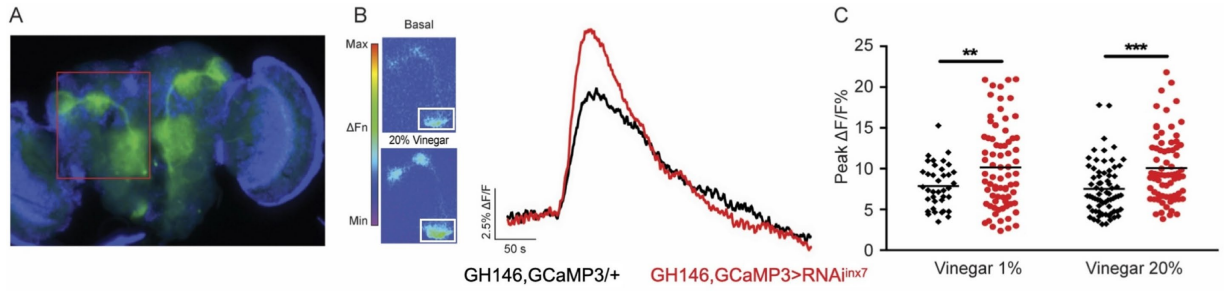

FIGURE 4
Inx7 knockdown affects vinegar-evoked calcium responses in AL PNs. **(A)** Fluorescent micrography showing the GCaMP3 expression confined to AL PNs using the Gal4 driver GH146. The red box shows GCaMP3 expression in AL glomeruli and projections to MB and lateral horn. **(B)** Vinegar exposure increases intracellular calcium concentration in AL PNs seen as an increase in fluorescence. The white square shows the ROI in the AL region where measurements were carried out. Representative traces of GCaMP3 fluorescence over time in AL glomeruli in response to 20% vinegar exposure are shown for control animals (GH146, GCaMP3/+, black trace) and flies expressing RNAi^{inx7} in AL PNs (GH146,GCaMP3 > RNAi^{inx7}, red trace). **(C)** Peak calcium signals evoked by 1 and 20% vinegar in AL in control and RNAi^{inx7}-expressing animals. An increase in both vinegar dilutions is observed upon Inx7 knockdown. ** and *** indicate $p < 0.01$ and $p < 0.001$, two-way ANOVA followed by Sidak's multiple comparisons test; n = 38–74 events per genotype, recorded from 5 or more different flies per condition.

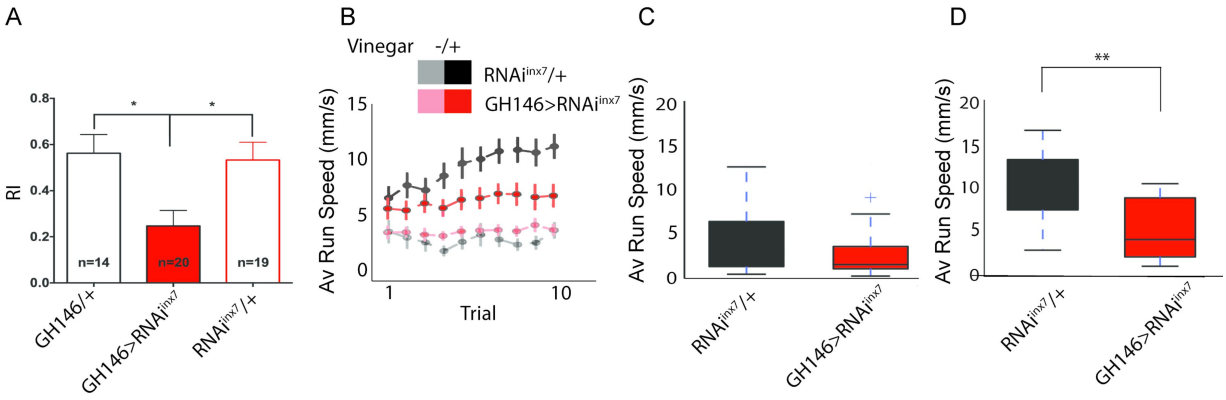

FIGURE 5
Behavioral responses to vinegar are affected in flies expressing an RNAi against *inx7* in AL PNs. **(A)** Groups of 30–50 control flies (GH146/+ or RNAi^{inx7}/+) show attraction toward vinegar, expressed as a positive index (RI) in a T-maze paradigm. Knocking down Inx7 in AL PNs (GH146 > RNAi^{inx7}) decreases RI. * indicates $p < 0.05$; one-way ANOVA followed by Dunnett's multiple comparisons test, n = number of flies tested, indicated for each genotype. **(B)** Individual, starved flies were acutely exposed to vinegar while the acute olfactive trail and locomotor behavior were recorded. This olfactory challenge was repeated 10 times consecutively. The average running speed per trial is presented for control and RNAi^{inx7}-expressing flies. An increase in this parameter is observed for the two strains only when vinegar is presented in the control flies (black vs. gray dots) and in the strain-expressing RNAi^{inx7} (red vs. light red dots). As the number of trials increases, an escalation in the speed is observed in the control strain (black dots), an effect that is not observed in the RNAi^{inx7}-expressing animals (red dots). No differences in the naïve locomotor response are observed in control or RNAi^{inx7}-expressing flies as the number of trials increases (light red vs. gray dots). **(C,D)** Comparison of the average speed for the 1st trial **(C)** and 10th trial **(D)**. No differences between controls and RNAi-expressing flies were observed in the first trial; however, differences were observed in the 10th trial **(D)**. ** indicate $p < 0.01$, Mann–Whitney U-test.

presented to the animals. Importantly, no difference in the response is detected in the first trial in the two strains (Figures 5B,C). Interestingly, in this paradigm, consecutive exposure to vinegar increases the speed of movement in control flies (Figure 5B, RNAi^{inx7}/+ group, black traces), a measure of increased motivation for food-seeking (Sayin et al., 2019). Remarkably, the flies expressing RNAi^{inx7} in AL PNs show no increased motivation for food-seeking when vinegar is repetitively presented, as no change in speed of movement is observed across the consecutive trials (Figure 5B, GH146 > RNAi^{inx7} group, red traces). Differences arose between the two strains and were evident after the 10th trial (Figure 5D). The difference between the strains cannot be explained by defects in basal locomotor performance in the RNAi^{inx7}-expressing flies, as naïve motor output is not affected in these flies when compared to control animals not exposed to the vinegar stimulus (Figure 5B, GH146 > RNAi^{inx7} and RNAi^{inx7}/+ groups, light red and gray traces; Supplementary Figure S2). This effect cannot be attributed to differences in the initial motivational state of RNAi^{inx7}-expressing flies compared to controls either, since no differences between the two strains are detected in the first trial (Figure 5C). Similar results are obtained using an Inx7 null mutant (Supplementary Figure S3).

These data demonstrate that Inx7 plays a key functional role in AL PNs in processing olfactory information that guides appetitive behaviors in adult *Drosophila*.

Discussion

Synchronization of activity between cells plays an important role in the coordination of responses to different stimuli in developing and mature olfactory systems. For instance, connexin36-containing gap junctions contribute to the synchronized activity between mitral and tufted cells in the OB, which is crucial for the organization, coordination, and processing of sensory olfactory information in vertebrates (Chen et al., 2009; Christie et al., 2005; Gire et al., 2012). Several reports show that gap junctions could play a similar role in the coordination of signals in the principal neurons of invertebrate AL, although the molecular determinants of such synchronization are not fully understood (Kazama and Wilson, 2009; Yaksi and Wilson, 2010; Huang et al., 2010).

Innexin 7 mediates PN-PN synchronized activity

Drosophila melanogaster has eight innexins, with ShakB (aka Inx8) being the most extensively studied regarding its contribution to gap junction formation and electrical communication in CNS neurons (Bauer et al., 2005; Beyer and Berthoud, 2018), particularly in the AL. For example, it is known that ShakB-containing gap junctions are necessary for correlated activity between PNs and excitatory LNs in the DA1 glomerulus in fly AL (Yaksi and Wilson, 2010) and also for the synergistic response observed when flies are exposed to a pheromone and an odorant signaling food (Das et al., 2017). Moreover, it has been shown that homotypic PNs (i.e., neurons within the same AL glomerulus) can form electrical synapses in *Drosophila* AL, which are mediated by ShakB (Yaksi and Wilson, 2010). Whether other innexins expressed in the AL also play a role in the synchronized activity is not known.

Here, we have shown that Inx7 expression is required for synchronized calcium activity between physically connected PNs *in vitro*. This suggests that PNs possess the ability to establish electrical synapses with other PNs via gap junction proteins such as ShakB or Inx7. Supporting this notion, Phelan et al. (2008) reported that ShakB expression is sufficient to promote gap junction formation between neighboring *Xenopus oocytes*. However, this may be more relevant for homotypic PN pairs, as the number of PN-GFP negative pairs with highly correlated calcium activity is smaller.

We detected a small number of PN-GFP-negative pairs that did show synchronized calcium activity. These GFP-negative neurons may represent unlabeled PNs, as previous studies have shown that the GH146-Gal4 driver does not label all PNs (Stocker et al., 1997). Alternatively, previous reports suggest that LNs also interact with PNs through chemical, electrical, and mixed electrochemical synapses, with all of these forms of neuron-to-neuron communication contributing to olfactory network activity in the *Drosophila* AL (Yaksi and Wilson, 2010; Huang et al., 2010). Thus, it is possible that in the culture system, the GFP-negative neurons correspond to AL LNs, which, in the fly brain, establish gap junctions with PNs.

We are aware that another possible explanation for our results is that innexins might form a different structure, namely hemichannels (HCs). HCs are assemblies of gap junction proteins located in the plasma membrane of a single cell (without physically communicating with another cell). HCs are molecular entities that allow the entry or exit of different molecules or ions in cells, and in that sense, they serve as a paracrine signaling mechanism (Abudara et al., 2018; Orellana et al., 2013). It has been shown that the activity of the HCs formed by Connexin43 plays an important role in modulating calcium dynamics in vertebrate cells, ultimately affecting calcium oscillations (De Bock et al., 2012; Turovsky et al., 2021). Considering this evidence, it is plausible to suggest that Inx7 forms HCs that, at least partially, contribute to the calcium transients and synchronized activity observed in AL PNs. Although there are some reports of the existence of HCs in cells of different insects (Luo and Turnbull, 2011; Yoshimura et al., 2020), including one in *Drosophila* (Prelic et al., 2024), to the best of our knowledge, HCs have not been shown to exist in neurons of any insects. Future studies should evaluate the existence of HCs in *Drosophila* neurons and investigate whether they modulate calcium dynamics in these cells.

Behavioral consequences of synchronized activity in AL

Electrical and/or calcium-synchronized activity has been associated with different functions in neurons and neural circuits (Melloni et al., 2007; Jutras and Buffalo, 2010; Uhlhaas and Singer, 2006). Notably, calcium oscillations in the insect MB have been suggested to be relevant to olfactory learning and memory (Rosay et al., 2001). Furthermore, spontaneous electrical activity has been observed in PNs in different invertebrates, where it appears to modulate the processing of olfactory information (Kazama and Wilson, 2009; Joseph et al., 2012). Although it is not clear what the role of AL oscillations is in odor processing, it has been proposed that they may help ensure the fidelity of information transmission within the olfactory circuit by refining the signal-to-noise ratio in downstream neurons such as KCs or lateral horn neurons (Kazama and Wilson, 2009; Joseph et al., 2012).

To advance our understanding of the contributions of PN gap junctions to odorant processing in *Drosophila*, we carried out functional imaging experiments using vinegar as an appetitive odorant. Exposure to this appetitive stimulus resulted in an increase in calcium activity in PNs in control flies. Interestingly, the calcium response in RNAi^{inx7}-expressing flies was higher compared to control flies. Similar results have been previously reported: exposure to some odorants evokes an increase in the firing rate in PNs of the VC1 glomerulus, which is further increased in the *shakB*^{2} loss-of-function mutant (Yaksi and Wilson, 2010). Thus, the expression of RNAi^{inx7} in AL PNs may lead to a decoupling of PN-PN pairs which, in turn, increases calcium activity in these neurons. However, our *in vitro* results do not support this idea, as calcium transients in AL PNs expressing RNAi^{inx7} are not different in frequency or amplitude from those recorded in single cultured AL PNs or in MB neurons *in vitro* (Jiang et al., 2005). Alternatively, one could propose that RNAi^{inx7} expression impairs the recruitment of inhibitory information to PNs across different glomeruli. Impairment of inhibitory information in PNs could affect the basal electrical properties of these neurons, making them more excitable. This idea is supported by the fact that inhibitory information is conveyed to PNs by LNs (Wilson and Laurent, 2005), as well as by previous studies showing that PN-LN electrical synapses are disrupted in mutants for the ShakB gap junction protein (Kazama and Wilson, 2009; Yaksi and Wilson, 2010).

The consequences of disrupting the Inx7-dependent gap junction in AL are evident as a reduced olfactory response to the attractive stimulus vinegar. Furthermore, we observed no change in the response

to successive vinegar exposures in RNAi^{inx7}-expressing flies. Functional integration of sensory information in an animal depends on different factors, such as the nature of the stimuli, the innate value of the information, and the inner state of the organism, among others. Our data show that consecutive vinegar exposure results in behavioral perseverance in control-starved flies, as previously described (Sayin et al., 2019). The perseverance is observed as an increase in average speed in starved flies after each trial in which they are exposed to vinegar. This increase in perseverance is not observed in RNAi^{inx7}-expressing flies, while basal locomotor responses to vinegar in starved flies are indistinguishable between RNAi^{inx7}-expressing and control flies. Thus, these data suggest a role for Inx7-based electrical synapses at the AL PNs in olfactory detection, which could have further consequences for the integration of sensory information related to the inner state of flies.

Overall, our results suggest that Inx7-based gap junctions are important contributors to the AL-synchronized activity underlying olfactory processing and responses in adult *Drosophila*.

Data availability statement

The raw data supporting the conclusions of this article will be made available by the authors, without undue reservation.

Ethics statement

The manuscript presents research on animals that do not require ethical approval for their study.

Author contributions

NF-U: Investigation, Writing – original draft. SH: Investigation, Writing – original draft. BS: Formal analysis, Investigation, Writing – original draft. SG: Formal analysis, Investigation, Writing – original draft. DV: Formal analysis, Investigation, Writing – original draft. PZ: Formal analysis, Investigation, Writing – original draft. TCH: Writing – review & editing. SS: Investigation, Methodology, Supervision, Writing – review & editing. IG: Methodology, Supervision, Writing – review & editing. DH: Investigation, Supervision, Writing – review & editing. DO'D: Conceptualization, Data curation, Formal analysis, Supervision, Writing – review & editing. JMC: Conceptualization, Formal analysis, Funding acquisition, Investigation, Project administration, Resources, Supervision, Writing – original draft, Writing – review & editing.

Funding

The author(s) declare that financial support was received for the research and/or publication of this article. This work was supported by FONDECYT grants 1231556 (to JMC); German Research Foundation (FOR2705, TP3); NRW network iBehave (to IGK); NIH R35 GM127102 (to TCH); ERC Starting Grant 101117267 (to DH); and NIH K99NS133470 (to SH).

Acknowledgments

We thank the members of our laboratories for their comments and ideas on this project. We would like to acknowledge the Bloomington *Drosophila* Stock Center for fly lines. We also thank the help of Margarita Meynard and Betty Sicaeros on the brain images and culture procedure, respectively. We are especially grateful to Dr. Sheeba Vasu for her support on *Drosophila* work and genetics. Jorge Campusano would like to dedicate this study to Professor Katia Gysling.

Conflict of interest

The authors declare that the research was conducted in the absence of any commercial or financial relationships that could be construed as a potential conflict of interest.

Generative AI statement

The author(s) declare that no Gen AI was used in the creation of this manuscript.

Publisher's note

Supplementary material

The Supplementary material for this article can be found online at: https://www.frontiersin.org/articles/10.3389/fncir.2025.1563401/full#supplementary-material

References

Abudara, V., Retamal, M. A., del Rio, R., and Orellana, J. A. (2018). Synaptic functions of Hemichannels and Pannexons: a double-edged sword. *Front. Mol. Neurosci.* 11:435. doi: 10.3389/fnmol.2018.00435

Ache, B. W., and Young, J. M. (2005). Olfaction: diverse species, conserved principles. *Neuron* 48, 417–430. doi: 10.1016/j.neuron.2005.10.022

Ammer, G., Vieira, R. M., Fendl, S., and Borst, A. (2022). Anatomical distribution and functional roles of electrical synapses in Drosophila. *Curr. Biol.* 32, 2022–2036.e4. doi: 10.1016/j.cub.2022.03.040

Bauer, R., Löer, B., Ostrowski, K., Martini, J., Weimbs, A., Lechner, H., et al. (2005). Intercellular communication: the Drosophila innexin multiprotein family of gap junction proteins. *Chem. Biol.* 12, 515–526. doi: 10.1016/j.chembiol.2005.02.013

Beyer, E. C., and Berthoud, V. M. (2018). Gap junction gene and protein families: Connexins, innexins, and pannexins. *Biochim. Biophys. Acta Biomembr.* 1860, 5–8. doi: 10.1016/j.bbamem.2017.05.016

Bracker, L. B., et al. (2013). Essential role of the mushroom body in context-dependent CO(2) avoidance in Drosophila. *Curr. Biol.* 23, 1228–1234. doi: 10.1016/j.cub.2013.05.029

Campusano, J. M., Su, H., Jiang, S. A., Sicaeros, B., and O'Dowd, D. K. (2007). nAChR-mediated calcium responses and plasticity in Drosophila Kenyon cells. *Dev. Neurobiol.* 67, 1520–1532. doi: 10.1002/dneu.20527

Chen, T. W., Lin, B. J., and Schild, D. (2009). Odor coding by modules of coherent mitral/tufted cells in the vertebrate olfactory bulb. *Proc. Natl. Acad. Sci. USA* 106, 2401–2406. doi: 10.1073/pnas.0810151106

Christie, J. M., Bark, C., Hormuzdi, S. G., Helbig, I., Monyer, H., and Westbrook, G. L. (2005). Connexin36 mediates spike synchrony in olfactory bulb glomeruli. *Neuron* 46, 761–772. doi: 10.1016/j.neuron.2005.04.030

Connors, B. W., and Long, M. A. (2004). Electrical synapses in the mammalian brain. *Annu. Rev. Neurosci.* 27, 393–418. doi: 10.1146/annurev.neuro.26.041002.131128

Curtin, K. D., Zhang, Z., and Wyman, R. J. (2002). Gap junction proteins expressed during development are required for adult neural function in the Drosophila optic lamina. *J. Neurosci.* 22, 7088–7096. doi: 10.1523/JNEUROSCI.22-16-07088.2002

Das, S., Trona, F., Khallaf, M. A., Schuh, E., Knaden, M., Hansson, B. S., et al. (2017). Electrical synapses mediate synergism between pheromone and food odors in Drosophila melanogaster. *Proc. Natl. Acad. Sci. USA* 114, E9962–E9971. doi: 10.1073/pnas.1712706114

De Bock, M., Wang, N., Bol, M., Decrock, E., Ponsaerts, R., Bultynck, G., et al. (2012). Connexin 43 hemichannels contribute to cytoplasmic Ca2+ oscillations by providing a bimodal Ca2+−dependent Ca2+ entry pathway. *J. Biol. Chem.* 287, 12250–12266. doi: 10.1074/jbc.M111.299610

Fabian, B., and Sachse, S. (2023). Experience-dependent plasticity in the olfactory system of Drosophila melanogaster and other insects. *Front. Cell. Neurosci.* 17:1130091. doi: 10.3389/fncel.2023.1130091

Fuenzalida-Uribe, N., and Campusano, J. M. (2018). Unveiling the dual role of the dopaminergic system on locomotion and the innate value for an aversive olfactory stimulus in Drosophila. *Neuroscience* 371, 433–444. doi: 10.1016/j.neuroscience.2017.12.032

Gire, D. H., Franks, K. M., Zak, J. D., Tanaka, K. F., Whitesell, J. D., Mulligan, A. A., et al. (2012). Mitral cells in the olfactory bulb are mainly excited through a multistep signaling path. *J. Neurosci.* 32, 2964–2975. doi: 10.1523/JNEUROSCI.5580-11.2012

Grabe, V., and Sachse, S. (2018). Fundamental principles of the olfactory code. *Biosystems* 164, 94–101. doi: 10.1016/j.biosystems.2017.10.010

Hidalgo, S., Campusano, J. M., and Hodge, J. J. L. (2021). Assessing olfactory, memory, social and circadian phenotypes associated with schizophrenia in a genetic model based on rim. *Transl. Psychiatry* 11:292. doi: 10.1038/s41398-021-01418-3

Huang, J., Zhang, W., Qiao, W., Hu, A., and Wang, Z. (2010). Functional connectivity and selective odor responses of excitatory local interneurons in Drosophila antennal lobe. *Neuron* 67, 1021–1033. doi: 10.1016/j.neuron.2010.08.025

Jefferis, G. S., Marin, E. C., Stocker, R. F., and Luo, L. (2001). Target neuron prespecification in the olfactory map of Drosophila. *Nature* 414, 204–208. doi: 10.1038/35102574

Jiang, S. A., Campusano, J. M., Su, H., and O'Dowd, D. K. (2005). Drosophila mushroom body Kenyon cells generate spontaneous calcium transients mediated by PLTX-sensitive calcium channels. *J. Neurophysiol.* 94, 491–500. doi: 10.1152/jn.00096.2005

Joseph, J., Dunn, F. A., and Stopfer, M. (2012). Spontaneous olfactory receptor neuron activity determines follower cell response properties. *J. Neurosci.* 32, 2900–2910. doi: 10.1523/JNEUROSCI.4207-11.2012

Jutras, M. J., and Buffalo, E. A. (2010). Synchronous neural activity and memory formation. *Curr. Opin. Neurobiol.* 20, 150–155. doi: 10.1016/j.conb.2010.02.006

Kay, L. M. (2015). Olfactory system oscillations across phyla. *Curr. Opin. Neurobiol.* 31, 141–147. doi: 10.1016/j.conb.2014.10.004

Kazama, H., and Wilson, R. I. (2009). Origins of correlated activity in an olfactory circuit. *Nat. Neurosci.* 12, 1136–1144. doi: 10.1038/nn.2376

Krashes, M. J., DasGupta, S., Vreede, A., White, B., Armstrong, J. D., and Waddell, S. (2009). A neural circuit mechanism integrating motivational state with memory expression in Drosophila. *Cell* 139, 416–427. doi: 10.1016/j.cell.2009.08.035

Leyton, V., Goles, N. I., Fuenzalida-Uribe, N., and Campusano, J. M. (2014). Octopamine and dopamine differentially modulate the nicotine-induced calcium response in Drosophila mushroom body Kenyon cells. *Neurosci. Lett.* 560, 16–20. doi: 10.1016/j.neulet.2013.12.006

Luo, K., and Turnbull, M. W. (2011). Characterization of nonjunctional hemichannels in caterpillar cells. *J. Insect Sci.* 11:6. doi: 10.1673/031.011.0106

Ma, J., and Lowe, G. (2010). Correlated firing in tufted cells of mouse olfactory bulb. *Neuroscience* 169, 1715–1738. doi: 10.1016/j.neuroscience.2010.06.033

Martin, J. P., Lei, H., Riffell, J. A., and Hildebrand, J. G. (2013). Synchronous firing of antennal-lobe projection neurons encodes the behaviorally effective ratio of sex-pheromone components in male Manduca sexta. *J. Comp. Physiol. A Neuroethol. Sens. Neural Behav. Physiol.* 199, 963–979. doi: 10.1007/s00359-013-0849-z

Melloni, L., Molina, C., Pena, M., Torres, D., Singer, W., and Rodriguez, E. (2007). Synchronization of neural activity across cortical areas correlates with conscious perception. *J. Neurosci.* 27, 2858–2865. doi: 10.1523/JNEUROSCI.4623-06.2007

Nagy, J. I., Pereda, A. E., and Rash, J. E. (2018). Electrical synapses in mammalian CNS: past eras, present focus and future directions. *Biochim. Biophys. Acta Biomembr.* 1860, 102–123. doi: 10.1016/j.bbamem.2017.05.019

Orellana, J. A., Martinez, A. D., and Retamal, M. A. (2013). Gap junction channels and hemichannels in the CNS: regulation by signaling molecules. *Neuropharmacology* 75, 567–582. doi: 10.1016/j.neuropharm.2013.02.020

Ostrowski, K., Bauer, R., and Hoch, M. (2008). The Drosophila innexin 7 gap junction protein is required for development of the embryonic nervous system. *Cell Commun. Adhes.* 15, 155–167. doi: 10.1080/15419060802013976

Phelan, P., Goulding, L. A., Tam, J. L. Y., Allen, M. J., Dawber, R. J., Davies, J. A., et al. (2008). Molecular mechanism of rectification at identified electrical synapses in the Drosophila giant fiber system. *Curr. Biol.* 18, 1955–1960. doi: 10.1016/j.cub.2008.10.067

Prelic, S., Keesey, I. W., Lavista-Llanos, S., Hansson, B. S., and Wicher, D. (2024). Innexin expression and localization in the Drosophila antenna indicate gap junction or hemichannel involvement in antennal chemosensory sensilla. *Cell Tissue Res.* 398, 35–62. doi: 10.1007/s00441-024-03909-3

Rojo-Cortes, F., Fuenzalida-Uribe, N., Tapia-Valladares, V., Roa, C. B., Hidalgo, S., González-Ramírez, M. C., et al. (2022). Lipophorin receptors regulate mushroom body development and complex behaviors in Drosophila. *BMC Biol.* 20:198. doi: 10.1186/s12915-022-01393-1

Rosay, P., Armstrong, J. D., Wang, Z., and Kaiser, K. (2001). Synchronized neural activity in the Drosophila memory centers and its modulation by amnesiac. *Neuron* 30, 759–770. doi: 10.1016/S0896-6273(01)00323-3

Sayin, S., de Backer, J. F., Siju, K. P., Wosniack, M. E., Lewis, L. P., Frisch, L. M., et al. (2019). A neural circuit arbitrates between persistence and withdrawal in hungry Drosophila. *Neuron* 104, 544–558.e6. doi: 10.1016/j.neuron.2019.07.028

Schoppa, N. E., and Westbrook, G. L. (2001). Glomerulus-specific synchronization of mitral cells in the olfactory bulb. *Neuron* 31, 639–651. doi: 10.1016/S0896-6273(01)00389-0

Semmelhack, J. L., and Wang, J. W. (2009). Select Drosophila glomeruli mediate innate olfactory attraction and aversion. *Nature* 459, 218–223. doi: 10.1038/nature07983

Stebbings, L. A., Todman, M. G., Phillips, R., Greer, C. E., Tam, J., Phelan, P., et al. (2002). Gap junctions in Drosophila: developmental expression of the entire innexin gene family. *Mech. Dev.* 113, 197–205. doi: 10.1016/S0925-4773(02)00025-4

Stocker, R. F., Heimbeck, G., Gendre, N., and de Belle, J. S. (1997). Neuroblast ablation in Drosophila P[GAL4] lines reveals origins of olfactory interneurons. *J. Neurobiol.* 32, 443–456. doi: 10.1002/(SICI)1097-4695(199705)32:5<443::AID-NEU1>3.0.CO;2-5

Stopfer, M., and Laurent, G. (1999). Short-term memory in olfactory network dynamics. *Nature* 402, 664–668. doi: 10.1038/45244

Strutz, A., Soelter, J., Baschwitz, A., Farhan, A., Grabe, V., Rybak, J., et al. (2014). Decoding odor quality and intensity in the Drosophila brain. *eLife* 3:e04147. doi: 10.7554/eLife.04147

Turovsky, E. A., Varlamova, E. G., and Turovskaya, M. V. (2021). Activation of Cx43 Hemichannels induces the generation of Ca2+ oscillations in White adipocytes and stimulates lipolysis. *Int. J. Mol. Sci.* 22:8095. doi: 10.3390/ijms22158095

Uhlhaas, P. J., and Singer, W. (2006). Neural synchrony in brain disorders: relevance for cognitive dysfunctions and pathophysiology. *Neuron* 52, 155–168. doi: 10.1016/j.neuron.2006.09.020

Vosshall, L. B., and Stocker, R. F. (2007). Molecular architecture of smell and taste in Drosophila. *Annu. Rev. Neurosci.* 30, 505–533. doi: 10.1146/annurev.neuro.30.051606.094306

Wilson, R. I., and Laurent, G. (2005). Role of GABAergic inhibition in shaping odor-evoked spatiotemporal patterns in the Drosophila antennal lobe. *J. Neurosci.* 25, 9069–9079. doi: 10.1523/JNEUROSCI.2070-05.2005

Wu, C. L., Shih, M. F., Lai, J. S., Yang, H. T., Turner, G. C., Chen, L., et al. (2011). Heterotypic gap junctions between two neurons in the drosophila brain are critical for memory. *Curr. Biol.* 21, 848–854. doi: 10.1016/j.cub.2011.02.041

Xie, Q., Brbic, M., Horns, F., Kolluru, S. S., Jones, R. C., Li, J., et al. (2021). Temporal evolution of single-cell transcriptomes of Drosophila olfactory projection neurons. *eLife* 10:e63450. doi: 10.7554/eLife.63450

Yaksi, E., and Wilson, R. I. (2010). Electrical coupling between olfactory glomeruli. *Neuron* 67, 1034–1047. doi: 10.1016/j.neuron.2010.08.041

Yoshimura, R., Suetsugu, T., Kawahara, A., Nakata, K., Shikata, M., Tanaka, S., et al. (2020). Formation of functional innexin hemichannels, as well as gap junctional channels, in an insect cell line, NIAs-AeAl-2, derived from Asian tiger mosquito Aedes albopictus (Diptera: Culicidae): a partial but significant contribution of innexin 2. *J. Insect Physiol.* 124:104060. doi: 10.1016/j.jinsphys.2020.104060